Picosecond X-Ray Diffraction Probed Transient Structural Changes in Organic Solids

S. Techert,[1,2,*] F. Schotte,[1] and M. Wulff[1]

[1]*European Synchrotron Radiation Facility, B.P. 220, F-38043 Grenoble Cedex, France*

[2]*Max-Planck-Institute for Biophysical Chemistry, Department 010, 37070 Göttingen, Germany*

(Received 16 May 2000)

In this Letter, we report on the experimental characterization of the geometry of short-lived electronically excited states in organic solids by time-resolved x-ray diffraction. Here, the structure factor of the organic crystal is measured as a function of time. Since this technique gives complete structural information, it is a very useful tool for learning more about atom motions on the excited-state energy surface—"beyond" the broad band typical of conventional spectroscopy. Although we used molecular crystals rather than free molecules, the compounds show detectable transient structural changes on the ps to ns time scale in our study.

DOI: 10.1103/PhysRevLett.86.2030 PACS numbers: 61.10.Eq, 78.47.+p

Introduction.—Since the discovery of fluorescence in charge-separated systems [1], considerable effort has been made to gain more insight into the interaction between geometrical changes and repulsive electronic effects on the excited state potential energy surface (PES). However, a disadvantage of conventional time-resolved (TR) spectroscopy is the lack of structural information. Since in these experiments the energetics of binding electrons are probed, it is impossible to deduce the atom positions during structural transitions without knowledge of the PES. Normally, the observed transient spectroscopic bands in the ultraviolet/visible range are very broad and even TR vibrational (IR) spectroscopy cannot cover the whole frequency range necessary for a complete structure determination [2]. Experimental results in ultrafast spectroscopy also raise the question whether ultrafast motions on the excited state PES can be described within the Born-Oppenheimer approximation [3] or whether one has to go beyond [4].

In this Letter, we describe an experimental approach using pulsed diffraction techniques for determining picosecond structures of photosensitive organic solids, where the structure factors of a system are measured as a function of time. The first nanosecond TR diffraction experiments were carried out at the European Synchrotron Radiation Facility (ESRF) with optical light as pump and polychromatic x-ray pulses from a synchrotron as probe on photoactive proteins such as the CO complex of myoglobin [5]. Recently, the time resolution has been improved by use of a mode-locked Ti:sapphire femtosecond laser which allows TR x-ray diffraction experiments down to 60 ps [6]. The principle of the experiment is summarized in Fig. 1, top: After photoinitiation of the reaction by a 150 fs optical laser pulse, the excited state is probed with a 100 ps x-ray pulse. By varying the delay between pump and probe, a series of snapshots of the moving structure can be taken where each shot probes the average structure (nonexcited and excited, including the dispersion of the latter) at a given time t_i. Since the typical lifetime of the systems reported here is in the nanosecond range, this is equivalent to following the structural relaxation pathways during the lifetime of the excited state—on the excited state PES. Apart from the improvement of the time resolution, this new setup can also run at a high repetition frequency of 897 Hz. Thus, it is now possible to accumulate monochromatic data on an integrating detector.

In this Letter, we study TR powder diffraction of *N*,*N*-dimethylaminobenzonitrile (DMABN, $C_9H_{10}N_2$, Fig. 1), a compound widely discussed in the literature with emphasis on relaxation mechanisms after photoexcitation [2,7–10]. It is also a special case of molecular charge transfer salt [11,12]. Our aim was to measure the structural relaxation following photoexcitation and to test the feasibility of using this method to determine displacements at atomic resolution on a picosecond time scale. One of the main questions was as follows: Does structural relaxation take place in a crystal and, if so, what are the amplitude and time scale (see Fig. 1, bottom)? With TR x-ray diffraction, it should be possible to distinguish between the inversion motion of the CH_3 groups around the N atom and the torsional motions of the CH_3 groups as relaxation processes on the excited state PES. Depending on the kind of motions, electronic coupling effects between the π electrons (torsion) or vibronic coupling as in NH_3 (inversion) characterize the photophysical behavior of DMABN.

Spectroscopic characterization.—From spectroscopic observations, some structural changes were expected even in light-activated DMABN crystals. Purified, recrystallized, and crushed samples were pressed in a gasket (sample diameter = 250 μm) until the 30 μm thick sample became optically transparent. The excitation and fluorescence spectra of the samples were recorded in the excitation/fluorescence mode of a commercial spectrometer (SPEX Fluorolog III, Jobin-Yvon). The spectra were found to be identical with published ones [13]. The biexponential fluorescence lifetimes of $\tau_1 = 1.71$ ns and $\tau_2 = 0.53$ ns at $\lambda_{emi} = 345$ nm were also observed [14]. In the present work, the lifetime of the excited state of DMABN crystals was determined to $\tau_f = 1.9$ ns (at

 0031-9007/01/86(10)/2030(4)$15.00

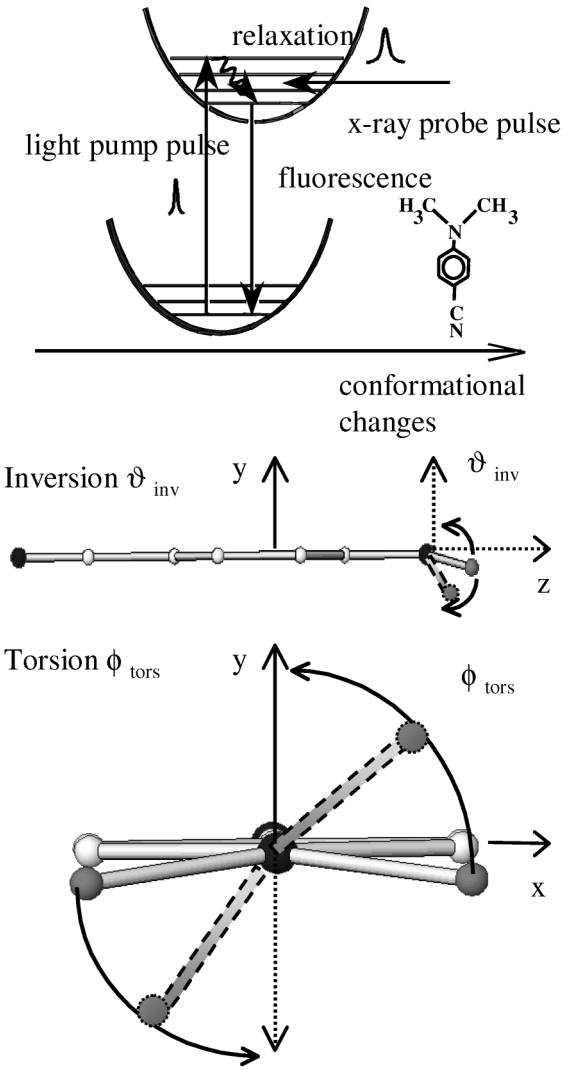

FIG. 1. Top: principle of TR x-ray diffraction on the excited-state PES of DMABN crystals. Bottom: the intramolecular degrees of freedom, which contribute to the relaxation process (inversion ϑ_{inv} and torsion ϕ_{tors}). C atoms of the phenyl moiety are given as open, N atoms as black, and the amino C as grey circles. Note that the H atoms are not shown, since they do not contribute to the x-ray diffraction signal.

$\lambda_{emi} = 375$ nm) by using a photon-counting instrument (Edinburgh Instruments, N_2 source with $\lambda_{exc} = 337$ nm, 500 ps resolution).

Data processing and structural refinement.—The data were collected on the ID09-TR beam line at the ESRF. A mode-locked Ti:sapphire laser [pulse width (laser) = 150 fs] runs synchronously with single pulses of x rays. A synchronized chopper was used to select the single x-ray pulses from the 16 bunches filling the storage ring [pulse width (x ray) = 100 ps, focus = 200×200 μm^2, flux on the sample = 8×10^7 photons/s. The polychromatic beam was produced by a 162 pole undulator with a 20 mm magnetic period ($K = 0.273$). The experiment used a monochromatic x-ray probe beam at 16.5 keV ($\lambda_{x\ ray} = 0.753$ Å) selected by a Si_{111} monochromator. High-resolution data sets were recorded using an image plate [size = 354×432 mm^2, pixel size = 100×100 μm^2, distance (sample detector) = 400 mm, exposure time = 1500 s]. Further data sets were collected with an image-intensified Princeton CCD camera [size = 124×115 mm^2, pixel size = 120×120 μm^2, distance (sample detector) = 80–150 mm, exposure time = 1200 s]. On the goniometer, the x-ray intensity of the direct beam was measured with a PIN diode before and after the measurement. During the measurement, the decay of the storage ring current was monitored on-line. Later, the collected spectra were intensity corrected. The pump wavelength was $\lambda_{exc} = 267$ nm (generated by frequency tripling, average power = 25–30 μJ, focus = 250 μm). The laser power of the direct beam was determined before and after every measurement and on-line monitored on a backscattered signal of a laser mirror. With 267 nm, DMABN was excited in the area of the highly vibrationally excited S_1 and the S_2 state. $t = 0$ was roughly set by using a fast Si avalange diode and double checked by monitoring the temporal change in the diffraction amplitudes of the sample. The accuracy of the time zero calibration was 30 ps, determined by the response function of the detector and its oscilloscope. The repetition frequency of the experiment was 897 Hz. The absorbed optical photons were partially emitted (with a fluorescence quantum yield of $\Phi_f = 0.3$) but also phonon-assisted emission at $\lambda_{emi} = 702$ nm was observed. The overall heating of the sample could be determined from the 2Θ shift of the Bragg peak maxima to $\Delta T = 2$ K. The laser and x-ray beams hit the sample in a quasiparallel configuration which gives the biggest overlap between pump and probe volume (see also [6]). The experiments were carried out at $T = 298$ K.

The collected powder patterns were integrated using the program FIT2D [15]. Subtracting the radial diffraction intensity between the (partially) excited and nonexcited state, one obtains—after suitable normalization—the intensity of the photoexcited state. Note that nonexcited unit cells do not contribute to the difference signal. Because of the reversible nature of the photoreaction, the nonexcited data could be taken at $t_i < 0$ where the laser arrived just before the x rays. Figure 2, top, shows the difference pattern $I(\Theta, t = 80\ \text{ps}) - I(\Theta, t = -240\ \text{ps})$. The $t = -240$ ps pattern contains the ground state $p1$. After laser excitation ($t = 80$ ps), the diffraction signal contains a mixture of ground state $p1$ and excited state $p2$. Figure 2, bottom, shows the change of the integrated Bragg peak intensities as a function of time. The Bragg reflections are marked by their Miller indices. The intensity change ranged between 1 ($\pm$0.5)–10 ($\pm$0.5)% of the total signal.

The structures were refined applying the Rietveld method (program package GSAS [16]). The powder data were analyzed in a biphasic model ($p1/p2$) keeping the phenylic moieties as rigid entities (rigid body approach [17]). The parameters of $p1$ were determined by the

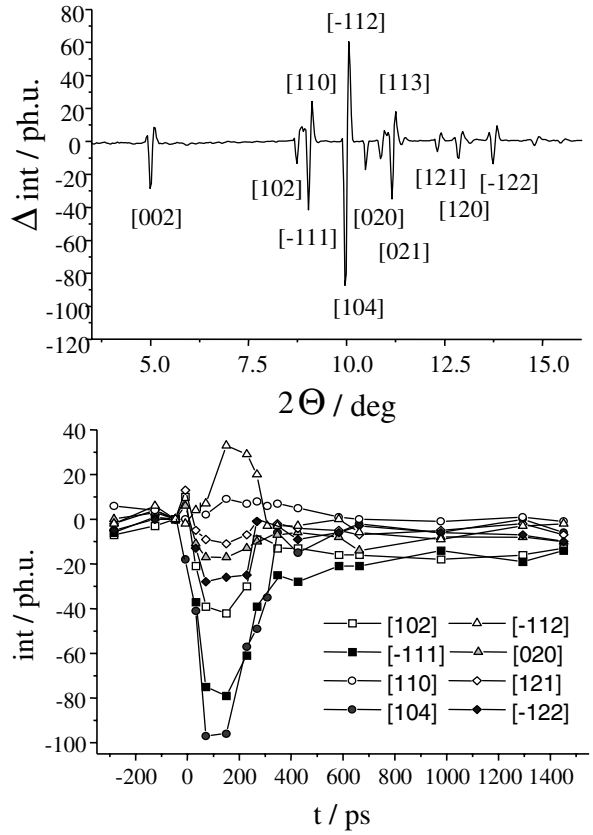

FIG. 2. Top: intensity difference map of the powder pattern at $t = 80$ ps and $t = -240$ ps. Bottom: change of the integrated Bragg intensities as a function of time. The intensity change ranges between 1%–10% of the total signal. Selected Bragg reflections are marked by their Miller indices.

refinement of the $t_i < 0$ structures. $p1$ is essentially the heated ground state structure [13,18]. The $t_i > 0$ structures were refined in $p2$ assuming a statistical distribution of the photoexcited molecules in the lattice. $p1$ acted as reference and was kept constant during analysis. In $p2$, the translational and rotational degrees of freedom (DOF) of the rigid body and the two intramolecular DOF, inversion and torsion (Fig. 1, bottom), were calculated and refined until a minimum in the least-square fit was reached. The quality of the least-square fits and the validity of the refined structure was expressed by the R factor which is defined by $R_F^2 = \Sigma|I_o - I_c|/\Sigma I_o$ (I_o = observed intensity at given Bragg angle, I_c = calculated intensity). The remaining intramolecular DOF (especially the benzonitrile- and N,N-dimethylamino moieties) were kept fixed during the refinements (for this widely used approach, see [19]). Based on the knowledge obtained, in particular, from TR-IR measurements [2], this assumption is reasonable since the distortions of the phenyl moiety in the singlet excited state as well as the distortions of the CN moiety were found to be negligibly small and not the driving forces of the photophysics of DMABN [2,20]. Since small distortions occur normally on extremely fast time scales, nuclear displacements of the benzonitrile moiety are to be expected on a femtosecond time scale and can therefore not be resolved in the experiment presented in this Letter. 450–500 observations were used and refined to the 12 structural DOF (four for the monoclinic unit cell, six for the rigid body molecule, and two for the molecular distortion).

The occupancies of $p1$ and $p2$ were also refined indicating the yield of photoexcited species compared to the ground-state species. For small t, the refined occupancies of $p2$, the photoexcited state, range from 28% to 32% and agree with the estimated excitation yield from spectroscopic data (25%–30%). However, the structural differences between $p1$ and $p2$ diminish for time points $t_i > 800$ ps leading to refined occupancies which might be meaningless.

DMABN crystallizes in a monoclinic space group $P\,2_1/c$ ($Z = 4$) [13,18]. The unit cell parameter was allowed to vary to compensate for small variations in the sample-to-detector distance [$a = 6.304$ (± 5) Å, $b = 7.941$ (± 3) Å, $c = 17.233$ (± 5) Å, and $\beta = 91.55$ (± 1.5)°]. A preferred orientation of the powder sample was excluded by comparing the intensity distribution of the various Bragg peaks and powder samples in rotated capillaries (where the microcrystals are assumed to be randomly orientated). No radiation damage—such as the increase of amorphous background or the gradual decrease of diffraction amplitudes—was observed.

Discussion.—The results of the experiments and the refinements are summarized in Table I. For $t_i < 0$ ps, the averaged inversion angle was found to be $\langle\vartheta_{\text{inv}}\rangle = 13\ (\pm 1)°$. After the absorption of an optical photon, the system is excited into the repulsive part of the PES of the excited state. Here, the structure reorganizes quickly from $\langle\vartheta_{\text{inv}}\rangle = 13\ (\pm 1)°$ to $\langle\vartheta_{\text{inv}}\rangle = 3\ (\pm 1)°$ bringing the system into a quasiplanar configuration (Table I, Fig. 3). Moreover, the CH_3 groups are rotated out of the benzylic plane: The averaged torsional angle increases from $\langle\phi_{\text{tors}}\rangle = 0\ (\pm 1)°$ to $\langle\phi_{\text{tors}}\rangle = 10\ (\pm 1)°$. If one compares $\langle\vartheta_{\text{inv}}\rangle$ and $\langle\phi_{\text{tors}}\rangle$ of the excited state in Table I with the

TABLE I. Geometries of different short-lived transient species of DMABN compared to high- and low-temperature structures. Five time points out of a series of 25 measurements are listed. T = temperature of the sample; t = time (error: ±30 ps); $\langle\vartheta_{\text{inv}}\rangle$ = averaged inversion angle (error: ±1%); $\langle\phi_{\text{tors}}\rangle$ = averaged torsional angle (amino moiety, error: ±1°); occ. = occupancy [%] (phase 2, error: ±4%), value in parentheses = fitting parameter (without physical meaning, see text); R_F^2, see text.

T	t	$\langle\vartheta_{\text{inv}}\rangle$	$\langle\phi_{\text{tors}}\rangle$	Occ.	R_F^2
301 K	static	10°	0°	100%	7.90% [13]
293 K	static	12°	0°	100%	4.31% [18]
173 K	static	7°	8°	100%	4.37% [13]
298 K	−240 ps	13°	0°	100%	6.40%
	80 ps	3°	9.5°	26%	4.89%
	240 ps	6°	8°	30%	5.25%
	470 ps	9°	6°	22%	4.80%
	1500 ps	14°	0°	(6%)	6.90%

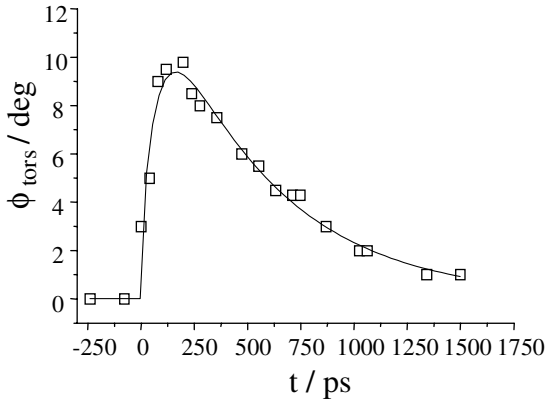

FIG. 3. Time evolution of the averaged torsional angle. A relaxation lifetime $\tau_{relax} = 520$ ps is observed (the electronic lifetime of the excited state of a molecule in the molecular crystal is $\tau_f = 1.7-1.9$ ns, this Letter and [14]).

known high- and low-temperature structures [13,18], the photoexcited structures resemble the low-temperature structure. This means that, during photoexcitation, DMABN "cools down" in terms of the structure, whereas the "structural cooling" is transient and nondissipative and concerns only the photoexcited molecules in the crystal (in contrast to [21]). However, the results can also be interpreted vice versa: It might be that the observed relaxation process is an effect of a complex coupling between the electronic and vibrational states, where the relaxation pathway of the electronically excited DMABN occurs via phonon scattering, which is shown in the distortion of the molecule. However, taking the size of the grains into account (about 5 μm^3), this effect is expected in 10–20 ns (further experiments and discussions will be given in [22]). Figure 3 shows the time dependence of $\langle \phi_{tors} \rangle$. The relaxation time $\tau_{relax} = 520$ ps is shorter than the electronic lifetime of the excited state of DMABN ($\tau_f = 1.9$ ns, this Letter and [14]). A more complex data analysis concerns the variation of the intermolecular parameters and will be presented in [22].

Summary.—In this Letter, we have reported on the structural characterization of ultrashort-lived organic crystals and their excited state geometry. Since these experiments require a high x-ray flux, the experiments were carried out using femtosecond laser pump and picosecond x-ray-probe pulses generated by a synchrotron of the third generation (ID09-TR at the ESRF in Grenoble). Though the work was done in crystals, on the picosecond to nanosecond time scale, the compounds showed transient structural changes which could be characterized by an ensemble of geometrical rearrangements during the relaxation processes. In DMABN, the excited state geometry is similar to the low-temperature structure. Interactions between the electronic and (intermolecular) vibrational states may also play a role as driving forces.

The authors thank M. Hanfland, H. Staerk, J. Troe, and K. A. Zachariasse for their support and the high interest in this work, which manifested itself in many useful discussions and comments.

*Author to whom correspondence should be addressed.
Electronic address: stecher@gwdg.de
Present address: Max-Planck-Institute for Biophysical Chemistry, Department 010, 37070 Göttingen, Germany.

[1] R. S. Mulliken, J. Chem. Phys. **7**, 121 (1939); R. A. Marcus, J. Chem. Phys. **65**, 679 (1965); A. Weller, Pure Appl. Chem. Phys. **16**, 115 (1968).
[2] C. Chudoba, A. Kummrow, J. Dreyer, J. Stenger, E. T. J. Nibbering, T. Elsaesser, and K. A. Zachariasse, Chem. Phys. Lett. **309**, 357 (1999).
[3] M. Born and R. Oppenheimer, Ann. Phys. (Leipzig) **84**, 457 (1928).
[4] H. Koeppel, W. Domcke, and L. S. Cederbaum, Adv. Chem. Phys. **57**, 59 (1984).
[5] D. Bourgeois, T. Ursby, M. Wulff, C. Pradevand, V. Srajer, A. LeGrand, W. Schildkamp, S. Laboure, C. Rubin, T.-Y. Teng, M. Roth, and K. Moffat, J. Synchrotron. Radiat. **3**, 65 (1996); V. Srajer, T.-Y. Teng, T. Ursby, C. Pradevard, Z. Ren, S. Adachi, W. Schildkamp, D. Bourgeois, M. Wulff, and K. Moffat, Science **274**, 1726–1729 (1996).
[6] F. Schotte, S. Techert, P. Anfinrud, V. Srajer, K. Moffat, and M. Wulff, in *Handbook of Synchrotron Radiation,* edited by D. Mills (Wiley, New York, 2000), Vol. 5.
[7] E. Lippert, Z. Naturforsch. **10A**, 541 (1955).
[8] K. Rotkiewicz, K. H. Grellmann, and Z. R. Grabowski, Chem. Phys. Lett. **19**, 315 (1973).
[9] W. S. Struve, P. M. Rentzepis, and J. Jortner, J. Chem. Phys. **59**, 5014 (1973); **60**, 1533 (1974).
[10] W. Rettig, Angew. Chem., Int. Ed. Engl. **25**, 971 (1986).
[11] S. Koshihara, Y. Tokura, K. Takeda, and T. Koda, Phys. Rev. Lett. **68**, 1148 (1992).
[12] *Relaxation of Excited States and Photoinduced Structural Phase Transitions,* edited by K. Nasu, Springer Series in Solid State Science Vol. 124 (Springer-Verlag, Berlin, 1997).
[13] G. B. Jameson, B. M. Sheikh-Ali, and R. G. Weiss, Acta Crystallogr. Sect. B **50**, 703 (1994).
[14] K. Rotkiewicz, H. Leismann, and W. Rettig, J. Photochem. Photobiol. A **49**, 347 (1989).
[15] A. P. Hammersley, M. Svensson, M. Hanfland, A. N. Fitch, and D. Haeussermann, High Press. Res. **14**, 235 (1996).
[16] A. C. Larson and R. B. von Dreele, *GSAS—General Structure Analysis System,* Program and Handbook, Los Alamos National Laboratory LAUR 86-748, California, (1998).
[17] P. Scheringer, Acta Crystallogr. **16**, 546 (1963).
[18] A. R. Heine, R. Herbst-Irmer, D. Stalke, W. Kuehnle, and K. A. Zachariasse, Acta Crystallogr. Sect. B **50**, 363 (1994).
[19] P. Lightfood, M. A. Metha, and P. G. Bruce, Science **262**, 883 (1993); R. E. Dinnebier, F. Olbrich, S. Van Smaalen, and W. Stephens, Acta Crystallogr. Sect. B **53**, 153 (1997).
[20] M. Grobys, K. A. Zachariasse, and E. Tauer, Chem. Phys. Lett. **274**, 365 (1997).
[21] C. E. Mungan, M. I. Buchwald, B. C. Edwards, R. I. Epstein, and T. R. Gosnell, Phys. Rev. Lett. **78**, 1030 (1997).
[22] S. Techert and M. Wulff (to be published).